---

**Article:**
Al-Khafaji, A, Neville, A orcid.org/0000-0002-6479-1871, Wilson, M orcid.org/0000-0002-1058-2003 et al. (1 more author) (2017) Effect of Low Salinity on the Oil Desorption Efficiency from Calcite and Silica Surfaces. Energy & Fuels, 31 (11). ISSN 0887-0624

https://doi.org/10.1021/acs.energyfuels.7b02182

---

# Effect of Low Salinity on the Oil Desorption Efficiency from Calcite and Silica Surfaces

Arije Al-Khafaji[1], Anne Neville[2], Mark Wilson[2], Dongsheng Wen[3]

[1] Chemical and Process Engineering Department, University of Leeds, Leeds, UK.

[2] Mechanical Engineering Department, University of Leeds, Leeds, UK.

[3] School of Aeronautic Science and Engineering, Beihang University, Beijing, 100191, China.

E-mail: D.Wen@leeds.ac.uk

## Abstract

Low salinity water flooding has been suggested to improve oil recovery in sandstone reservoirs. However, application in carbonate reservoirs is still controversial. In this work, Quartz Crystal Microbalance (QCM-D) was used to investigate the impact of the chemical composition of crude oils and crystal surfaces on the adsorption/desorption efficiency of oil components upon exposure to various salinity solutions to reveal the potential of enhancing oil recovery from carbonate reservoirs. The surface charge of carbonate rock is characterized by zeta potential measurements. For QCM-D measurements, Norwegian and North Sea crude oils with various acid numbers were used, while calcite and silica crystals were utilized to mimic carbonate and sandstone reservoirs. The results reveal that the amount of adsorption is correlated to the concentration of polar organic components present in the oil and the type of surface mineral. Subsequent desorption showed that low amounts of desorption are reported upon exposure to seawater for both surfaces examined, while two and ten times diluted seawater achieved the highest desorption efficiency. These observations are supported by zeta potential measurements for carbonate rock and previous electrokinetic studies for silica surfaces. Generally, increasing the content of negative polar components in crude oil leads to a reduced desorption from calcite surface compared to the silica surface. Low salinity water flooding seems not to be an

optimal technique to improve oil recovery from carbonate reservoirs with high acidity and heavy crude oil.

## 1. Introduction

Throughout the years, various enhanced oil recovery techniques have been developed, especially in the last two decades. Low salinity flooding has been proposed as an innovative method to improve oil recovery (IOR) in hydrocarbon reservoirs. A broad range of studies have been conducted recently to study the effect of low salinity water flooding in sandstone reservoirs and identify the potential recovery mechanisms. The laboratory observations supported by limited field scale tests have shown that lowering the salinity of water below 5000 PPM could produce positive results for sandstone reservoirs [21,25,31-32,34,40,43,46-48,52]. However, it is worthwhile to mention that, the effect of low salinity water flooding on carbonate rocks remains controversial and its application in the field scale is still doubtful. The reason behind this is the complex chemical interactions between brine/ carbonate rock/ and crude oil, which lead to a poor understanding of the chemical mechanisms responsible for oil recovery improvement [12,18].

Various mechanisms have been proposed in the literature to elucidate the brine/oil/carbonate rock interactions during low salinity flooding, but none of them are commonly accepted. A multiple ion exchange mechanism has been suggested by Austed et al. [7], who found that the presence of the $SO_4^{2-}$ ion and a reduced concentration of NaCl, combined with the optimum temperature, i.e. between 90-110 ℃, are necessary to change the we ttability of carbonate reservoirs, which can then affect the total recovery. In addition, the theory of the electrical double layer (EDL) expansion has been proposed as one of the other mechanisms that could lead to improved oil recovery during low salinity injection [33]. It proposes that when the rock surface is exposed to a low saline solution, the EDL is formed due to the ion exchange between a charged rock surface and an electrolyte solution. Consequently,

the interaction between the EDL and the oil-brine interface help to detach hydrophobic layers from the surfaces, which can contribute to the wettability alteration of carbonate rocks to a favorable state [30].

On the other hand, it has been reported that the amount of polar organic components present in crude oil strongly affects the potential of low salinity flooding for both carbonate and sandstone rocks [8, 39]. Hence, the adsorption of these compounds from crude oil onto rocks is considered an essential pre-condition for the influence of low salinity flooding to enhance oil recovery [43]. Polar compounds consist of both acidic components, including carboxylic and phenolic acids, and basic components such as nitrogen compounds [10,41]. A number of studies indicated that the acid/base content from asphaltenes and resin fractions in crude oil have a major effect on the wettability alteration of mineral surfaces [8,11,13,35].

QCM has been extensively used to detect the adsorption and interactions of polymers at solid/liquid interfaces. For instance, Guo and colleagues [20] investigated the adsorption behavior of two cationic polyelectrolytes that have different charge densities on silica and gold surfaces. The results revealed that the adsorption of the polyelectrolyte relies on the solid surface, solution concentration and solution pH. Li et al. [26] also studied the adsorption behaviors of four thermo-sensitive triblock copolymers in dilute aqueous solutions on hydrophobic modified gold surface at various temperatures. They found that the adsorption time constant decreased with increasing adsorption temperature. The adsorption/desorption of asphaltene and its fractions onto silica surfaces has also been evaluated by the Quartz Crystal Microbalance (QCM) technique as a simple and quick method compared to the classical core flooding process [12,13,36]. Recently QCM has been used to assess the adsorption/desorption of crude oil on different surfaces [14,15,48]. However, there are very few studies carried out to address the crude oil adsorption/desorption onto/from carbonate mineral surfaces.

From the aforementioned research, it is clear that understanding the effect of low salinity water flooding and the exact mechanisms causing oil mobilization are very limited for carbonate reservoirs. Assessing the adsorption/desorption efficiency will be helpful to explain the complex oil/brine/ carbonate rock interactions and evaluate the potential of low salinity flooding. This work aims to conduct a fundamental study of how the ionic strength and brine salinity influences the desorption of crude oil with different chemical compositions from crystal surfaces. Three crude oils with various acid number have been studied, while calcite and silica coated QCM crystals were used to simulate carbonate and sandstone rocks. The surface charge (i.e., electrostatic force) of pure calcite minerals upon exposure to different salinity solutions are identified. The role of polar organic components associated with the acidity of oil and its effect on the crude oil adsorption/desorption efficiency onto/from calcite and sandstone surfaces are examined.

## 2. Materials and Methods

### 2.1 Rock Sample

Homogenous Estaillades limestone outcrop rock was used in zeta potential measurements. The core samples were supplied by Shell. The average porosity and permeability of Estaillades core are 25 % and 100 md, respectively. The average grain density is 2.74 g/cc, measured by Micromeritics Acupyc-1330. X-ray Diffraction (XRD) analysis was carried out by an XRD Bruker D8 Diffractometer to quantify the mineral composition of the limestone rock. The results reveal that the powder of crushed limestone rock was composed of mainly (94 %) calcite with a small amount (6%) of Dolomite. No clay minerals were detected in the sample (see Figure 1).

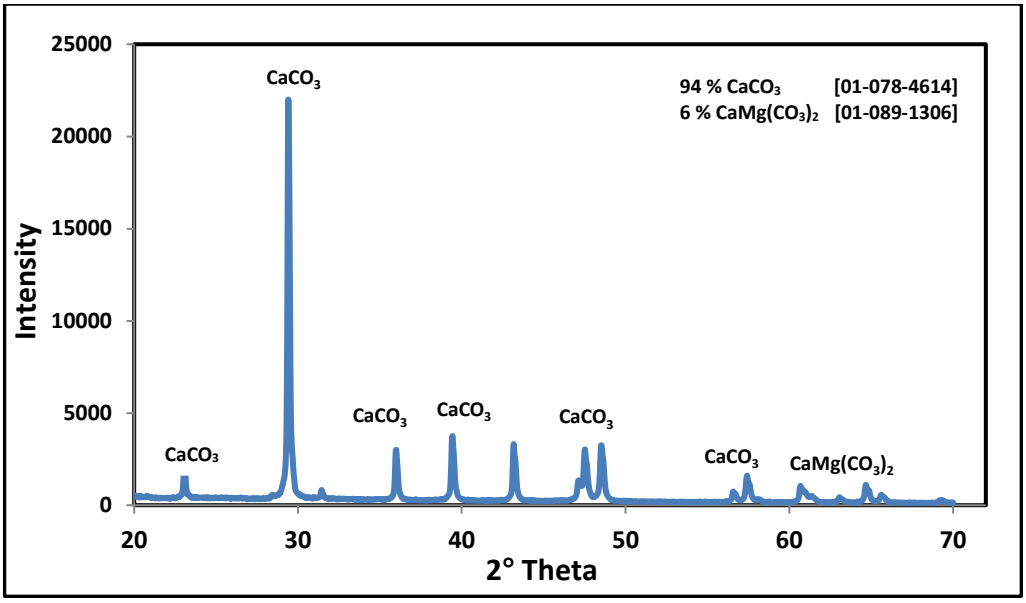


**Figure 1. XRD response of Estaillades limestone rock.**

2.2 Calcite and Silica Sensors

CaCO3 (QSX 999) and SiO2 (QSX 303) standard coated sensors were purchased from Q-Sense Biolin Scientific. The sensors consist of a quartz crystal disk with metal electrodes on each side. One of the electrodes was covered with thin surface layers to simulate either carbonate or sandstone minerals. The fundamental resonant frequency for the crystals is 5 MHz.

**2.3 Brines**

In this study, synthetic seawater (SW) and artificial formation water (FW) were used as the base brines. All brines were prepared in the lab by mixing deionized water (Milli-Q, resistivity >18.2 MΩ.cm) with reagent grade salts, which were supplied by Merck and Sigma with a purity grade > 99%. The artificial low salinity (LS) solutions were made by diluting the prepared seawater with different proportions of deionized water. This includes twice-diluted seawater (2dSW), 5 times-diluted seawater (5dSW), 10 times-diluted seawater (10dSW), 20 times-diluted seawater (20dSW) and 50 times-diluted seawater (50dSW), See Table 1. The synthetic saline solutions used in the

experiments are displayed in Figure 2. The physical properties of all prepared brines were characterized by measuring density, viscosity, conductivity, and pH. Table 2 illustrates the details of physical properties for different brines.

**Table 1. The composition of high salinity and low salinity brines**

| Salts | FW | SW | 2dSW | 5dSW | 10dSW | 20dSW | 50dSW |
|---|---|---|---|---|---|---|---|
| NaCl | 124.5 | 26.5 | 13.25 | 5.3 | 2.65 | 1.33 | 0.53 |
| $Na_2SO_4$ | 0.43 | 4.10 | 2.05 | 0.82 | 0.41 | 0.20 | 0.08 |
| $CaCl_2.2H_2O$ | 57.79 | 1.54 | 0.77 | 0.31 | 0.15 | 0.08 | 0.03 |
| $MgCl_2.6H_2O$ | 16.87 | 11.41 | 5.70 | 2.28 | 1.14 | 0.57 | 0.23 |
| $NaHCO_3$ | 0.40 | 0.11 | 0.05 | 0.02 | 0.01 | 0.005 | 0.002 |
| TDS (g/L) | 200 | 43.65 | 21.82 | 8.73 | 4.37 | 2.18 | 0.873 |
| Ionic strength (ppm) | 200000 | 43650 | 21828 | 8731 | 4366 | 2183 | 873 |

**Table 2. Physical properties of high salinity and low salinity brines**

| Brines Types | Ionic strength (ppm) | Density ($gm/cm^3$) | Viscosity [a] (cp) | Conductivity (mS/cm) | pH |
|---|---|---|---|---|---|
| FW | 200000 | 1.18865 | 1.995 | 149.2 | 6.7 |
| SW | 43650 | 1.04394 | 1.142 | 42.70 | 7.96 |
| 2dSW | 21828 | 1.04138 | 1.125 | 16.17 | 7.58 |
| 5dSW | 8731.2 | 1.03875 | 1.012 | 8.80 | 7.34 |
| 10dSW | 4365.6 | 1.03579 | 1.002 | 4.97 | 7.24 |
| 20dSW | 2182.8 | 1.02848 | 0.989 | 2.77 | 7.15 |
| 50dSW | 873.12 | 1.009 | 0.936 | 1.11 | 7.01 |

[a] Values were determined at a shear rate region between (10-1000) 1/s.


**Figure 2. Synthetic formation water, seawater, and different diluted versions of seawater.**

## 2.4 Crude Oils

Three kinds of dead crude oil were supplied by Lundin and Shell companies from oil fields in Alta and the North Sea, respectively. A Malvern Bohlin Rheometer and Micromeritics Acupyc-1330 were used to measure viscosity and density. SARA fractionation was used to analyze the bulk composition of oils with respect to saturates, aromatics, and asphaltenes. The mass ratios of N, S, and O were determined by an Elemental Analyzer (Thermo EA2000). The physiochemical properties of the crude oils are given in Table 3.

**Table 3. Physiochemical properties of crude oils**

| Specification | Crude Oil A | Crude Oil B | Crude Oil C |
|---|---|---|---|
| Specific gravity at 25 ℃, gm/cm $^3$ | 0.827 | 0.835 | 0.933 |
| ºAPI | 39.5 | 38 | 20 |
| Dynamic viscosity at 20 ℃, cp | 5.5 | 7.4 | 50 |
| Dynamic viscosity at 50 ℃, cp | 2.94 | 4.5 | 28 |
| Total acid number (TAN), mg KOH/g at 25 ℃ | 0.25 | 0.46 | 2.54 |
| **Composition (wt%) at 25 ℃** | | | |
| Saturates | 73.7 | 64.53 | 32.25 |
| Aromatics | 22.75 | 28.81 | 44.91 |
| Asphaltenes | 0.21 | 0.47 | 11.13 |
| **Elemental analysis (wt%) at 25 ℃** | | | |
| Nitrogen | 1.14 | 0.88 | 1.06 |
| Sulphur | 0 | 0.19 | 0.32 |
| Oxygen | 2.2 | 5.12 | 10.33 |
| **Remarks** | Low acid number | Moderate acid number | High acid number |

## 2.5 Zeta Potential Measurements

A Colloidal Dynamics Zeta-Probe was used to determine the zeta potential of different calcite-brine suspensions, which is an accurate instrument based on electro-acoustic measurements without the need for sample dilution**.** It measures the dynamic mobility of charged colloidal suspensions at different frequencies in the MHz range.

To prepare suspensions, 2% weight of calcite powder was added to various brine solutions under magnetic stirring to maintain homogeneity and left one day to reach equilibrium. The particles size distribution was then determined using Malvern Mastersizer-2000E. The mean size of the grains did not exceed 3 μm for all investigated suspensions. Figure 3 shows a typical example of the grains size distribution in seawater. It is obvious that the calcite particles have a median size of 2.5 μm. This can provide a way of proper dispersing in the aqueous phase and satisfy the range of zeta potential measurements. It is also worth pointing out that the calcite particles aging in different suspensions have similar specific surface area (SSA), ranging between 1.9 and 2.3 $m^2/g$, determined by Quantachrome Nova 2200. A typical scanning electron microscope (SEM) was also used to image the calcite particles before and after exposure to various salt solutions. From Figure 4A, the calcite particles show anisotropic microstructure and heterogeneity in the grain size. Aging calcite particles in twice-diluted seawater solution revealed a change in morphology of the grains, which can be related to the presence of adsorbed salt ions on the surface (Figure 4B).

The zeta potential measurements of the various calcite-brine suspensions were conducted at a constant pH value of 8, typical of carbonate reservoir conditions. 0.1 mole/L for HCl and NaOH solutions was used to adjust the pH of suspensions. All zeta potential measurements were conducted at 25 ℃. Three runs were carried out for each sample with f ive cycles' measurement for each run, and an average value of zeta potential was evaluated within this range. The standard deviation of repeated zeta potential measurements is about 0.5 mV.

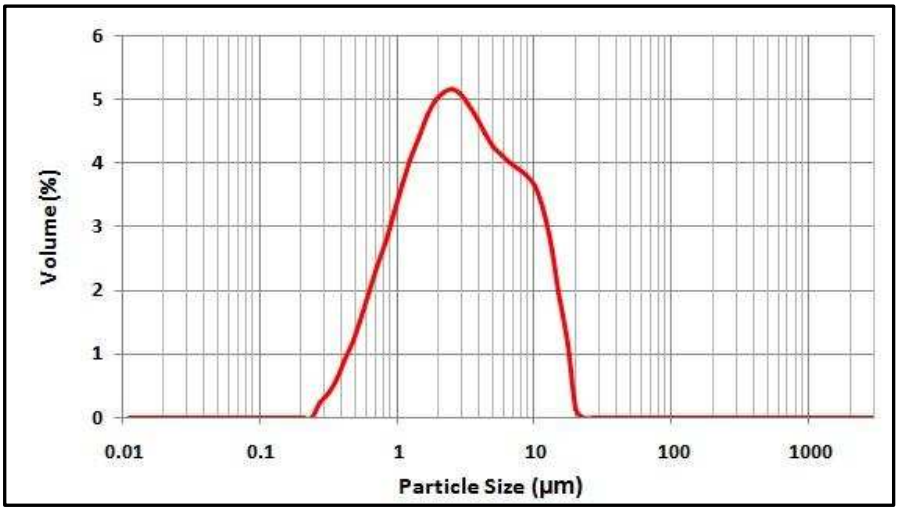


**Figure 3. Particles size distribution of calcite in seawater**.

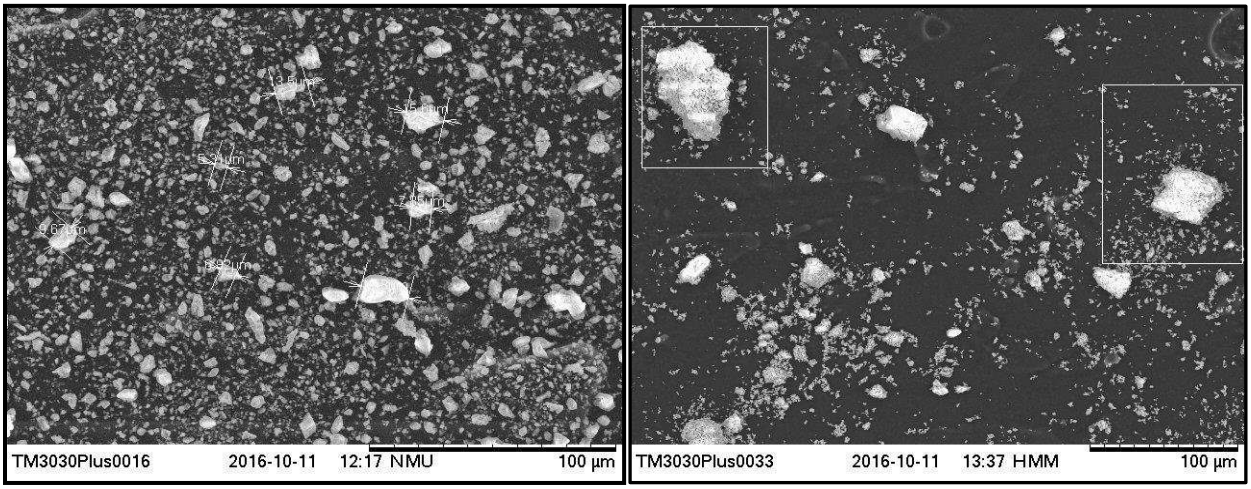


**(A)** **(B)**

**Figure 4. SEM image of A) fresh calcite particles. B) calcite particles treated with 2 times diluted sea water.**

## 2.6 Quartz Crystal Microbalance (QCM) Measurements

In this work, a Q-Sense D300 was used to detect the adsorption/ desorption of crude oil onto/from the calcite and silica coated crystals. Q-Sense measures the change in resonant frequency and dissipation energy of the coated crystals used. The change in frequency when the oscillating crystal

is exposed to an aqueous phase can be attributed to the mass loading, liquid loading, and liquid trapping. The adsorbed mass of a thin and rigid adhering layer is determined by the Sauerbrey equation (Eq.1) [38]. When Newtonian fluids come into contact with the oscillating crystal, an additional shift in frequency is observed due to the change in density and/or viscosity of the medium (Eq.2) [22]. The liquid trapping effect can be neglected because of the atomic smoothness of the crystal surfaces. The principle calculations of mass and liquid loading are described by the following equations:

$$\Delta f_{ads.} = -\frac{n\ r_{QCM}}{C} \quad \textbf{(1)}$$

$$\Delta f_{liq.load} = -\sqrt{\frac{nf^3}{\pi\rho_q\, \upsilon_q}}\left(\sqrt{\rho_1\ \eta_1} - \sqrt{\rho_2\ \eta_2}\right) \quad \textbf{(2)}$$

where $r_{QCM}$ is the adsorbed mass (mg/m$^2$), $n$ is the harmonic number, C is the constant of quartz crystal (0.177 mg/m$^2$ Hz), $f^3$ is the fundamental frequency of the crystal (5 MHz), $\rho_q$ is the specific density of quartz (2650 kg/m$^3$), $\upsilon_q$ is the shear wave velocity in quartz (3340 m/s), $\rho$ is the density of solution, kg/m$^3$, and $\eta$ is the viscosity of solution, kg/m.s. Subscription 1 and 2 refer to the solutions of different densities and viscosities.

To perform the experiments, the calcite sensor was utilized to mimic the pure calcite minerals of the natural carbonate rock, used in the zeta potential measurements. Whereas, silica sensor was used to represent sandstone rock. Prior to each experiment, the sensor was immersed in 2 wt. % Hellmanex cleaning solution for 30 minutes, then washed several times with Milli-Q water to get the cleanest possible surface. Afterwards, the sensor was blow-dried with air duster removal and put in a UV-ozone chamber for 10 minutes. The chemical resistant tubes and QCM chamber were also cleaned with Iso-Propanol and Milli-Q water many times to remove any organic contamination. All adsorption /desorption QCM experiments were conducted at 22 ℃.

In order to get a stable baseline, toluene was first injected. This was achieved by flushing toluene into the chamber for 20 minutes until the oscillation in frequency was about ± 2 Hz. After that, 2mL of dead crude oil was injected by gravitative flow into the chamber. After oil saturated the crystal surface and equilibrium was reached (30-50 minutes), toluene was injected again to detach loosely held oil components. Next, a high salinity solution represented by sea water was injected. Finally, different diluted versions of seawater were flooded sequentially through the QCM chamber. When the frequency was stabilized for each particular solution (20-25 min), the changes in frequency were detected. The amount of desorbed oil after exposure to different aqueous salt solutions was calculated by the difference between the measured frequency shift and liquid loading shift due to the difference in densities and viscosities i.e, $\Delta f_{des} = \Delta f_{measured} - \Delta f_{liquid\ load}$. The desorption efficiency was calculated by (desorbed mass/adsorbed mass) x100. The measurements were repeated three times for each type of crude oil to ensure the accuracy and reliability of the results. The relative standard deviation of repeated measurements was less than 5%.

## 3. Results and Discussion

### 3.1 Zeta Potential

The zeta potential of calcite particles in deionized water was examined first over a wide range of pH (6.5-11.5) as a reference test. From Figure 5, it can be clearly seen that positive zeta potential values were reported throughout the pH range covered. This might be commonly linked to the high concentration of the $Ca^{2+}$ ion in the surface lattice (crystal structure). This trend is in line with the study of Kasha et al. [24] for a dolomite-deionized water suspension. In addition, a high pH would increase the concentration of $CO_3^{2-}$, $HCO^-_3$, and $OH^-$ [19,30], leading to a less positive charge. Thus, as illustrated in Figure 5, the magnitude of the positive surface charge is decreased clearly (from +17.27 mV to +3.2 mV) with an increase of pH value, making the surface less positive.

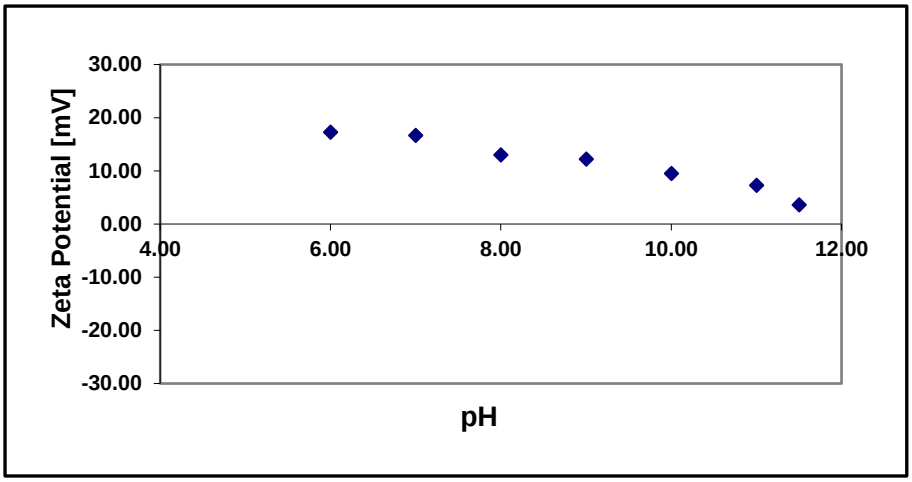


**Figure 5. Zeta potential of calcite particles in deionized water.**

Figure 6 shows the zeta potential values of calcite particles in formation water, sea water, and different dilutions of sea water at pH 8. It can be seen that the zeta potential of calcite particles was positive (+10.37 mV) in formation water which represents the highest brine concentration (200000 ppm) used in this study. This result is consistent with the findings from Mahani et al. [30] that the zeta potential for the different types of carbonate particles in high salinity water is positive due to the high concentration of ($Ca^{2+}$ and $Mg^{2+}$) ions, leading to a shrinkage of the EDL and shift of the zeta potential to a positive value. In comparison, the zeta potential in sea water was less positive than formation water (+3.6 mV) at the same pH value. This could be attributed to the reduction in the total dissolved solids (43650 ppm) and an increase of the concentration of the $SO_4^{2-}$ ion in sea water, which is consistent with the previous studies [23,24].

The results also reveal that the magnitude of the negative charge generally increases as the salinity and ionic strength of suspensions decreases up to 10 times dilution. For instance, the zeta potential of calcite particles in twice-diluted sea water is -5.12 mV, and it reaches to -10.6 mV at 10 times dilution. It is logical that as the salinity of suspension decreases, the adsorption of $Mg^{2+}$ and $Ca^{2+}$ ions surrounding the particles decreases with continuous adsorption of $SO_4^{2-}$. This leads to the expansion of the EDL and an increase in the magnitude of the negative surface charge [30]. However,

further brine dilution causes more reduction in the concentration of $SO_4^{2-}$ and therefore less negative charge is observed, i.e., a zeta potential of -3.24 mV is obtained at 50 times dilution. Al Alotaibi et al. [2] also confirmed that less negative charges were observed by using aquifer water without sulphate at certain pH. It is also worthwhile to mention that because of the calcite particles have small specific area (1.9-2.2 $m^2/g$), we expect that the reaction surface will be small, and therefore less zeta potential values compared to the other types of carbonate rock have been reported. A study performed by Vdovic [45] showed that a significant difference in the zeta potential values was observed for the two synthetic calcite samples, having different surface area. His conclusion is that the specific surface area and grain size could affect the magnitude of electric charge or energy stored on the calcite surface.

For silica surfaces, the zeta potential measurements have not been performed in this study for technical reasons and the results of the previous work have been considered to analyze the brine/silica/oil interactions in the next sections. Many previous electrostatic studies showed that silica surfaces have an isoelectric point at PH 2 and the surface will be more negative at PH >6 [5,17,29]. AlQuraishi and his colleagues [4] also stated that a substantial increase in the magnitude of the negative surface charges of sandstone rock was observed when switching from seawater to 2 times dilution of seawater and then to 10 times dilution, respectively. In the same way, the zeta potential of clay minerals and sandstones in aquifer water, seawater, and deionized water has been studied by Al Alotaibi et al. [3]. Their results showed a negative zeta potential for all samples examined, and the highest negative charges were for sandstone in deionized water followed by chlorite particles in aquifer water. Such results indicate that the silica surface is almost negatively charged under low salinity solutions.

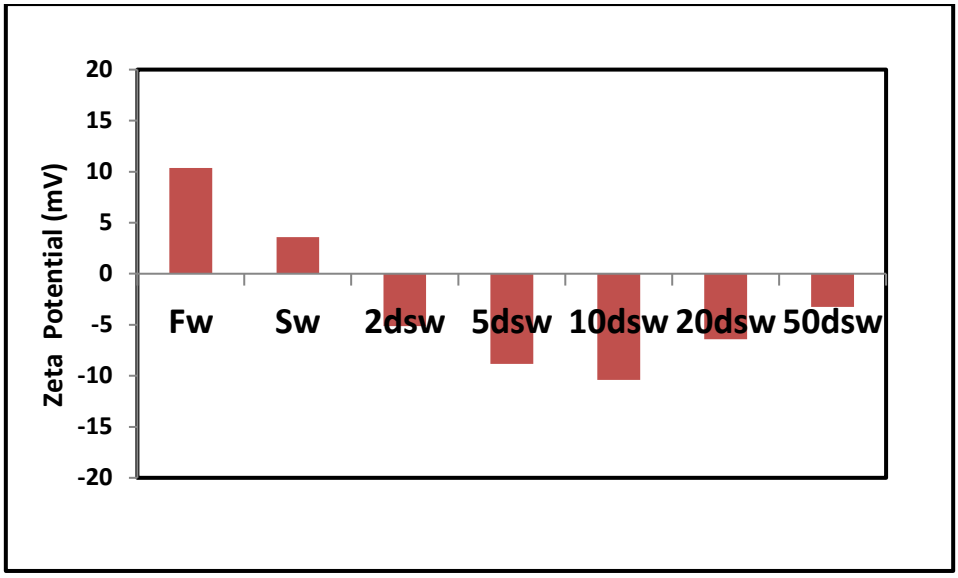


**Figure 6. Averaged zeta potential of calcite particles in high and low salinity solutions at pH 8.**

### 3.2 Adsorption of Crude Oil on Calcite and Silica Surfaces

An indicative example of the frequency and dissipation changes when calcite and silica surfaces are exposed to dead crude oil, followed by flushing with toluene and subsequent exposure to seawater and different slugs of diluted seawater, is illustrated in Figure 7. It is obvious that a frequency shift on the silica surface is higher than that on the calcite surface, suggesting that the mass adsorbed rapidly on the surface [15]. These results are in line with those of Guo et al. [20], who noted that a higher shift in the frequency was on the silica surface than that on the gold surface. They stated that silica ($SiO_2$) has higher electrostatic contact sites compared to the other surfaces, leading to more molecules adsorbed on the $SiO_2$ surface through the electrostatic attraction. It can also be seen from Figure 7 that the corresponding dissipation shift increases during the adsorption of crude oil onto the investigated surfaces, but it decreases upon exposure to toluene, meaning that loosely bound oil molecules were detached from the surface and the residual components represent a rigid oil layer [35]. It can also be noted that injecting 2dSW and 10dSW show an increase in the frequency shifts, coinciding with a decrease in the corresponding dissipation shifts, indicating that a desorption

happened as will be discussed in the next section. Moreover, the overall dissipation shifts for the calcite and silica surfaces are relatively small (less than 10). Similar behaviors have been observed previously [15,26,35,44].

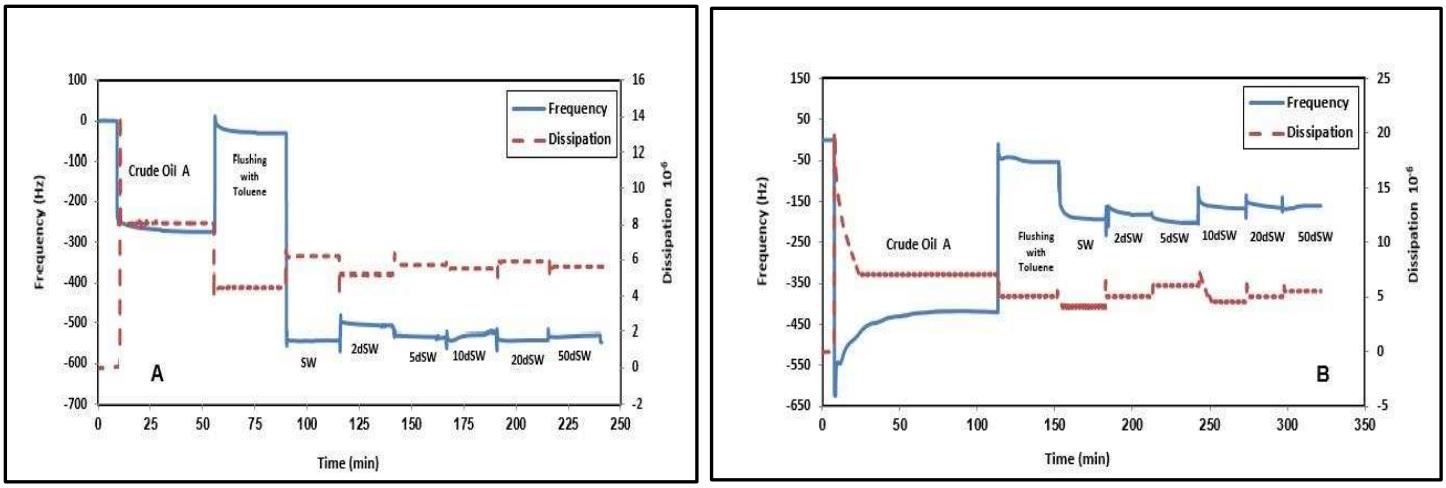


**Figure 7. Frequency and dissipation shifts (third overtone) versus time for typical adsorption/desorption sequences onto (A) calcite and (B) silica surfaces.**

The adsorbed mass was determined by the Sauerbrey equation Eq. (1) and the results are shown in Figure 8. For calcite surfaces, the highest adsorption was observed for crude oil C, which contained a high acid number (2.54 mg KOH/g) and the highest mass ratio of oxygen atom (see Table 3). On the other hand, the lowest adsorption was for crude oil A with no significant acidity and less oxygen content. For silica surfaces, an opposite trend is observed since the adsorption is decreased as the acidity of crude oil and oxygen hetero atom increased. This observation is consistent with the study from Liu et al. [29], who confirmed that the oil components adsorbed to silica surfaces were different from those on calcite surfaces.

Based on the fact that silica surface is dominated by silanol (Si-OH) groups, the surface will be negatively charged, which can promote the adsorption of positively charged nitrogen based components present in oil

[5,8,35]. It might be speculated that more layers are adsorbed to silica surfaces compared to calcite surfaces when crude oils with insignificant acidity have been used (Crude Oil A and B). Overall, the variation in the amount of mass adsorbed can be attributed to the difference in the chemistry of the oil adsorbed.

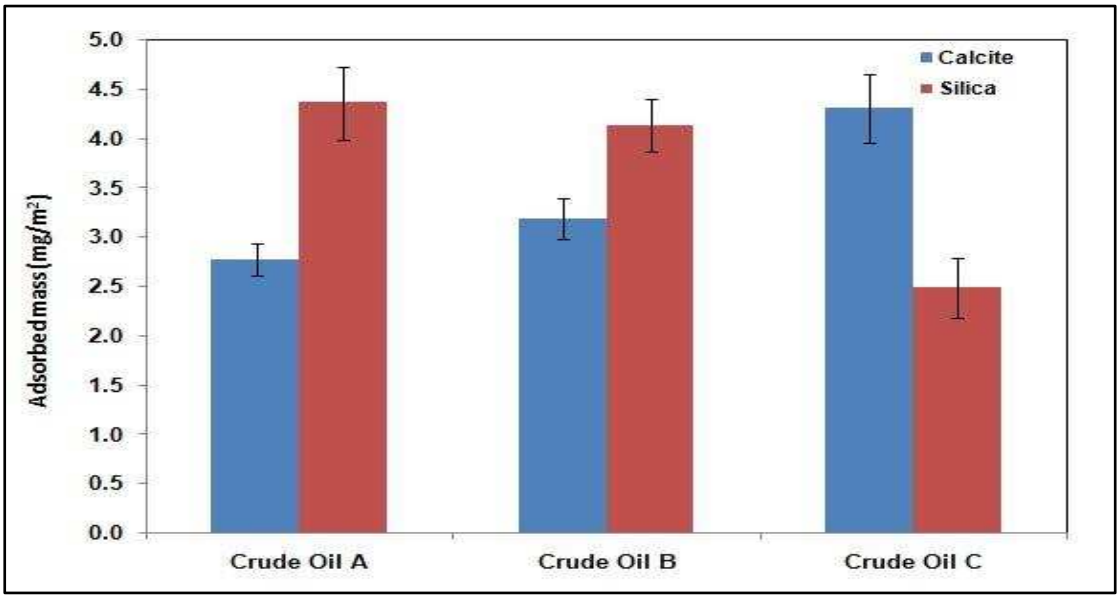


**Figure 8. Amount of adsorbed crude oils on the calcite and silica surfaces.**

To support the above-mentioned observations, Infra-Red Spectroscopy (FTir-Thermo iS10) was used to determine the organic functional groups present in the crude oils. The IR spectra obtained for three crude oil samples are illustrated in Figure 9. Considering the functional groups of crude oils, it can be seen that the absorption bands of aliphatic hydrocarbon ($CH_2$ and $CH_3$) represent the major functional groups in crude oils A, B and C, including C-H stretching of the saturate (2800-2921 $cm^{-1}$), C-H deformation of saturate (1455.25 $cm^{-1}$) and C-H symmetric deformation of saturate (1376.56 $cm^{-1}$) [37]. The region between (1640-1737 $cm^{-1}$) was consistent with the stretching carboxylic groups C-O, such as carboxylic acid. This region depicted two small peaks for crude oil C, which showed the highest adsorption on the calcite surface, referring to the presence of the C-O functional group in this

kind of oil. The peak at (1141.6 $cm^{-1}$) in crude oil A and B was assigned to the presence of amine C-N stretch.

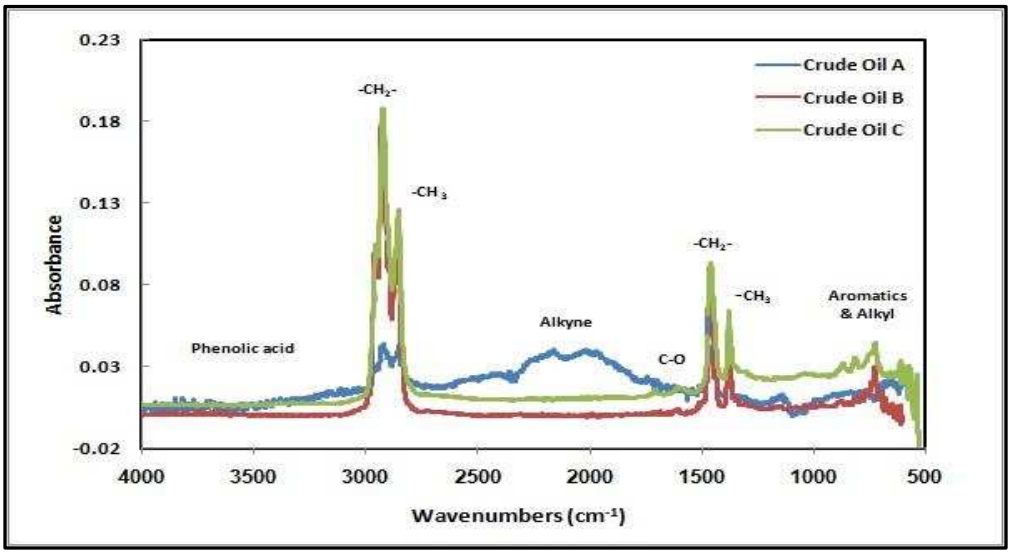


**Figure 9. Infra-Red spectra of the three crude oils used in this study.**

The results also revealed that the three crude oil samples contain an amount of phenolic functional groups in the range of (3107-3938 $cm^{-1}$). Finally, the wave number in the range between (1505.6-1538. $cm^{-1}$) corresponded to aromatics ring stretch C-C, while the band between (800-600 $cm^{-1}$) was assigned to the aromatics C-H deformations and alkyl groups [35]. Notably, the aromatic bands were more intense for crude oil C, which give an indication of high aromaticity for this sample compared to crude oils A and B. SARA analysis also confirmed that crude oil C has a high aromatic weight ratio 44.91%.

In general, IR spectra indicate that the saturated hydrocarbon bands seem to be the predominant function groups for all types of crude oils. However, there is variation in the abundance of polar groups such as carboxylic acid, amine, and phenolic acid. IR spectroscopy observations have also been supported by SARA and elemental analyses, which showed equivalent contents of saturate and polar hetero atoms groups (NO). These results were consistent with the amount of adsorbed oil layers on the calcite

and silica surfaces. It has previously been reported that the surface energy seems likely to be dominated by the basic, acidic and polar components of the oil adsorbed, and the crude oil solvent character with respect to its polar components have a considerable impact on deposition or precipitation at the solid surface [9,29].

### 3.3 Desorption of Crude Oil from Calcite and Silica Surfaces

The desorption efficiency of oils from calcite and silica surfaces upon exposure to various salinity solutions was calculated, as shown in Figures 10 and 12. The desorption efficiency is generally decreased as the acidity of crude oil is increased. From Fig. 10, the lowest desorption efficiency was for crude oil C, which contained the highest acidic components (O= 10.33%). Whereas the highest desorption efficiency was for crude oil A, having the lowest amount of acidic components (O= 2.2%). These observations could be attributed to the high bonding strength of negatively charged acidic components onto the positively charged calcite surface. It has been reported that a very limited change in wetting conditions was observed at the acid number larger than 1 [42]. Fathi et al. [17] also found that the oil depleted in water-soluble acids can be displaced easily from the chalk cores compared to the original oil with a high acid number (1.8 mg KOH/mg).

Injecting seawater showed some desorption of the adsorbed layer from calcite surface, and not much difference in desorption efficiency was observed for various types of oils used. This result may originate from the mutual interactions between sulphate ion adsorbed ($SO_4^{2-}$) and calcium ion ($Ca^{2+}$), i.e., multiple ion exchange on the surface, could be happening. The mutual interactions therefore could improve the electrostatic repulsion between the adsorbed polar oil components and calcite surface, thereby resulting in desorption from the calcite surface [6,42]. The reactivity of $Mg^{2+}$ ion could also increase in water and it can even substitute $Ca^{2+}$ from the calcite surface and thereby displace $Ca^{2+}$ ions that are bridged to carboxylic polar components, leading to further desorption from the carbonate surface. Figure 11A illustrates the potential chemical interactions between calcite/crude oil and

saline solution. It is worth commenting that imbibition and core flooding experiments emphasized that seawater removed some of the light and heavy crude oils from carbonate rocks during secondary flooding [21,42,50-52].

Furthermore, the significant desorption occurred when the calcite surface with adsorbed oil layer is subjected to solutions of 2dSW and 10dSW, sequentially. These results are qualitatively in good agreement with our findings of zeta potential mentioned earlier in section 3.1. When the salinity decreased, the surface potential of the calcite became more negatively charged. As the adsorbed oil layer is also negatively charged due to the presence of negative polar active components, it can lead to an increase in the electrostatic repulsion and an improvement in the desorption efficiency. Conversely, a very small desorption was noticed with further dilution (20dSW and 50dSW) as further dilution displays less negative zeta potential, Figure 6.

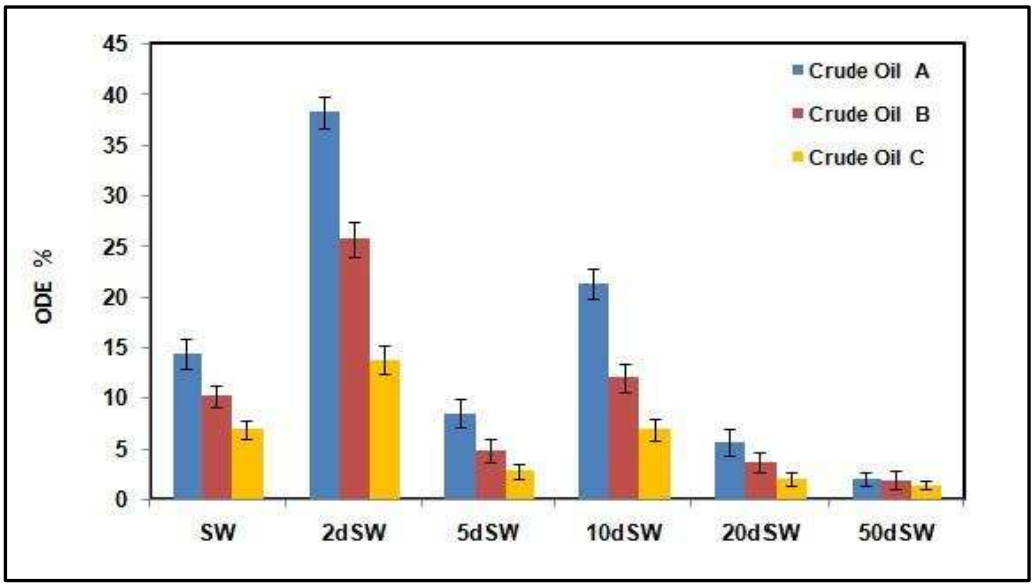


**Figure 10. Oil desorption efficiency from the calcite surface upon exposure to seawater and different diluted versions of seawater.**

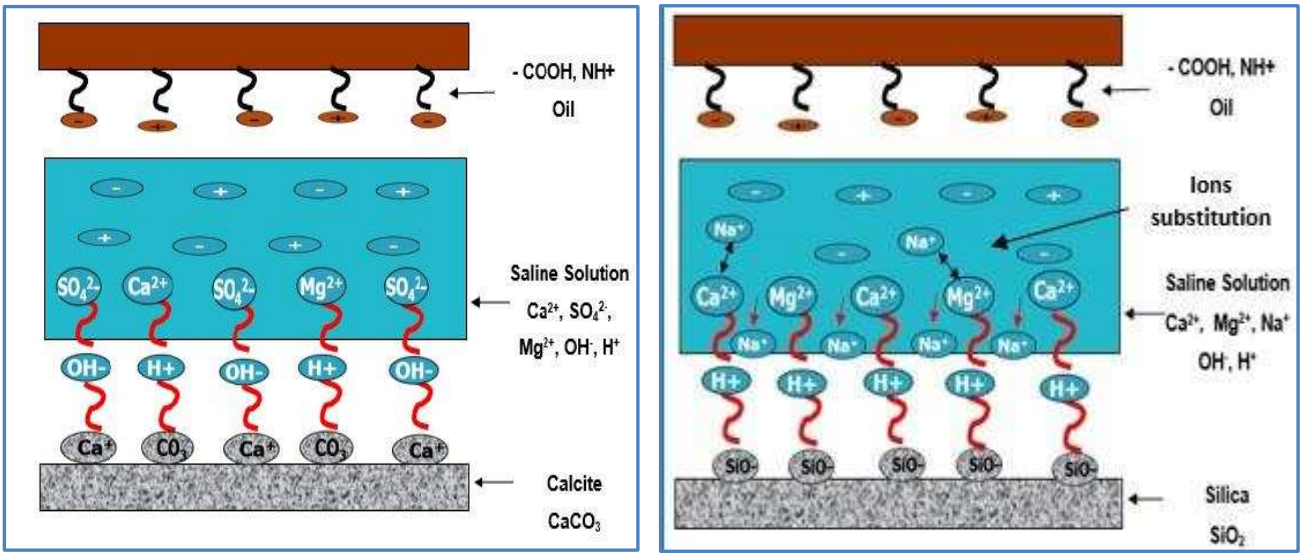


**(A)** **(B)**

**Figure 11. Potential interactions between calcite/silica and oil components upon exposure to saline solution.**

In the case of silica, Figure 12 shows that there is less amount of the adsorbed oil was desorbed than from the calcite surface at the high salinity solution (seawater). Previous studies have suggested that both oil and solid interfaces become charged in the presence of water film [8]. Hence, injecting high salinity solution with the presence of positive divalent ions such as $Ca^{2+}$ and $Mg^{2+}$ can act as a bridge between dissociated negative polar oil components and negative silica surface sites, leading to adverse desorption (See Figure 11B). These results are consistent with the basis of the experimental work of Lager and his coworkers [25] that a conventional high salinity waterflood containing the high concentration of $Ca^{2+}$ and $Mg^{2+}$ resulted in low recovery factor compared with the modified brine (depleted in $Ca^{2+}$ and $Mg^{2+}$). Considering the bridging effect of potential determining ions, we can thus expect limited desorption (4%) of crude oil C, which has the highest polar component, from silica surface upon exposure to seawater.

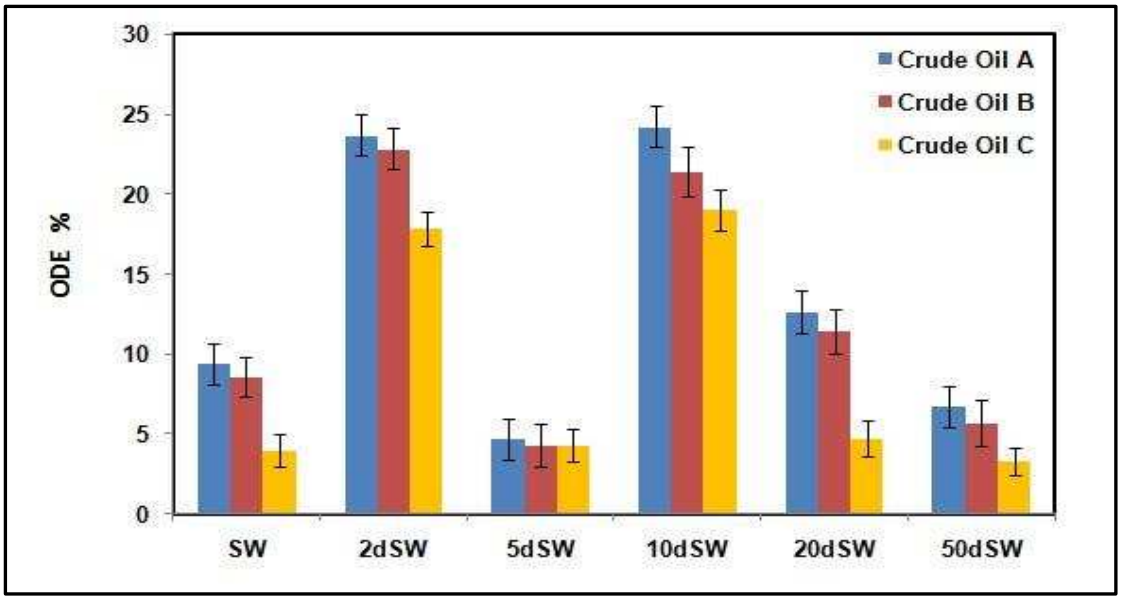


**Figure 12. Oil desorption efficiency from the silica surface upon exposure to seawater and different diluted versions of seawater.**

On the other hand, it is obvious from Figure 12 that injecting low salinity solution increases the extent of desorption from silica surface in comparison with high salinity solution. The highest desorption efficiency is observed for 10 times-diluted seawater. It is apparent that a sharp decrease in the attraction force was happened when switching from seawater to 10dSW. This could be explained by DLVO theory and/or ion binding mechanism. In our system, the interactions occurred between the silica coated sensor and crude oil in the presence of the aqueous phase. It has previously been suggested that the isoelectric point for silica is about pH 2 and the surface is negatively charged at neutral pH [5,29]. As illustrated in Table 2, the low salinity solutions have a pH range from 7.01-7.58, which can increase the negative charge on surface sites. Thus, at the low electrolyte concentration and a relatively high surface charge density, the repulsive energy of the electrical double layer is going to play a vital role in the interactions between oil/brine/silica interfaces, and therefore promoting the desorption efficiency when a solution of 10 times dilution used. In contrast, injected seawater is likely to screen of the surface charges, resulting in a decrease in the repulsion and less desorption efficiency. A further limited desorption has been observed at 50dSW. In this case, despite the ionic strength of salt solution being

reduced at neutral pH value, the repulsive electrostatic force is likely to be insufficient to promote the desorption. Farooq et al. [15] found that a critical expansion of the EDL is required for further desorption from silica by low salinity solution.

Another possible explanation in which the saline solutions impact the desorption of crude oil from silica surface is by considering the effect of mutual ion interaction, as the divalent cations ($Ca^{2+}$ and $Mg^{2+}$) could be replaced by the monovalent cations, such as $Na^{+}$ (see Figure 11B). As a result, the divalent ions leave the silica surface along with the crude oil [9]. This could provide further proof to explain the limited desorption when utilizing 20 and 50 times-diluted seawater, i.e, when the ionic strength was decreased. The only opposite trend is for 5dSW, and the reason for this behavior could be related to the reduction in the effect of the ions binding and EDL expansion. As with the 5 times dilution, the concentration of the divalent and monovalent ions is relatively decreased and correspondingly, their binding to the solid/water interfaces is reduced. Simultaneously, in comparison with the 10dsw, we expect that the electrical double layer expansion is not large enough to promote the desorption of oil. This means that the two proposed mechanisms are not much dominant for the oil desorption when 5dSW used.

For different diluted versions of seawater, the overall desorption from silica surface was the highest for crude oil A with the low polar contents, acid number= 0.25 mg KOH/g. As illustrated in Figure 11B, the presence of electrolyte solutions results in the formation of a positively charged water film between silica and oil. Therefore, if we consider the crude oil with a higher acid number (crude oil C), then the acidic components are tightly held through water phase, thereby resulting in less desorption [1]. Generally, the effect of active polar components present in crude oil on the oil desorption efficiency (ODE) is more pronounced for calcite surface than silica surface upon exposure to various salinities. This discrepancy may be because of the difference in electrostatic interactions between charged functional groups in oil and charged mineral surfaces.

## 4. Conclusions

In this study, the impact of ionic strength and brine salinity on the electrokinetic behavior of carbonate rock is investigated, as well as the adsorption/desorption efficiency of various types of crude oils onto calcite and silica surfaces under different aqueous phases is evaluated. The overall zeta potential measurements demonstrate that as the salinity and ionic strength of suspensions decreases up to 10 times dilution, the magnitude of the negative charges increases. The results of adsorption by QCM-D show that more oil layers are adsorbed on the calcite surface when the acidity of oil is increased, while the opposite trend was observed for silica surface. This suggests that the amount of adsorbed layer depends mainly on the composition of oil and the surface mineral type.

Less desorption happens from silica surface compared to calcite surface upon exposure to seawater for all three oils examined. Twice-diluted seawater and 10 times diluted seawater give high desorption efficiency for both surfaces examined because of increasing the repulsion forces between adsorbed polar organic components and surfaces. The results also suggest that either EDL expansion (electrokinetics repulsive) or multiple ion exchange mechanism alone could affect the desorption efficiency, i.e., a combination of these two mechanisms are dominant for the oil desorption. Nevertheless, it is important to emphasize here that which of these two mechanisms considered the main governing factor for the oil desorption is hard to detect.

Furthermore, the effect of active polar components representing by the acid number on the oil desorption efficiency (ODE) is more pronounced for calcite surface than for silica upon exposure to different salinity solutions. Thus, low salinity solution may not be an optimal choice for removing acidic crude oil from calcite surfaces.

## References


1. Abdolmohsen, S.A, Ayoub, M.A, Saaid, I.M Experimental Investigation into Effects of Crude Oil Acid and Base Number on Wettability Alteration by Using Different Low Salinity Water in Sandstone Rock. Journal of the Japan Petroleum Institute 2015, 58(4) 228-236.

2. Alotaibi, M.B and Nasr-El-Din, H.A. Electrokinetics of Limestone and Dolomite Rock Particles. SPE Reservoir Evaluation and Engineering 2011,594-603.

3. Alotaibi, M.B and Nasr-El-Din, H.A. Wettability Studies Using Low-Salinity Water in Sandstone Reservoirs. SPE Reservoir Evaluation and Engineering 2011,713-725.

4. AlQuraishi, A.A., AlHussinan, S.N., and AlYami, H.Q Efficiency and Recovery Mechanisms of Low Salinity Water Flooding in Sandstone and Carbonate Reservoirs. SPE Offshore Mediterranean Conference and Exhibition, Ravenna, Italy, 2015.

5. Anderson, A. & William, G. Wettability Literature Survey-Part 1: Rock/Oil/Brine Interactions and the Effects of Core Handling on Wettability. Society of Petroleum Engineer 1986, 38 (11), 1125-1127.

6. Austad , T., Strand, S., Høgnesen, E.J., Zhang, P. Seawater as IOR Fluid in Fractured Chalk, SPE International Symposium on Oil field Chemistry, Society of Petroleum Engineers Inc, The Woodlands, Texas 2005.

7. Austad, T., Shariatpanahi, S.F., Strand, S., Black, C.J.J, and Webb, K.J. Conditions for a Low-Salinity Enhanced Oil Recovery (EOR) Effect in Carbonate Oil Reservoirs. Energy & Fuels 2012, 26, 569-575.

8. Buckley, J.S and Liu,Y. Mechanisms of Wetting Alteration by Crude Oils. Journal of Petroleum Science and Engineering 1998, 3 (1),54-61.

9. Buckley, J.S and Liu,Y. Some Mechanisms of Crude/Brine/Solid Interactions. Journal of Petroleum Science and Engineering, 20,1996, 155-160.

10. Buckley, J.S Mechanisms and Consequences of Wettability Alteration by Crude Oils. Doctoral Thesis. Heriot Watt University 1996.

11. Clementz, D.M. Alteration of Rock Properties by Adsorption of Petroleum Heavy Ends: Implications for Enhanced Oil Recovery, SPE Enhanced Oil Recovery Symposium, Tulsa, April 4-7, 1982.

12. Doust, A. R., Puntervold, T., Strand, S. and Austad, T. Smart Water as Wettability Modifier in Carbonate and Sandstone: A Discussion of Similarities/Differences in the Chemical Mechanisms. Energy & Fuels 2009, 23, 4479-4485.

13. Dubey, S.T. and Doe, P.H. Base Number and Wetting Properties of Crude Oils. SPE Reservoirs Engineering 1993, 8 (3),195-200.

14. Ekholm , P., Blomberg, E., Claesson, P., Auflem, IH., Sjöblom, J. and Kornfeldt, A. A Quartz Crystal Microbalance Study of the Adsorption of Asphaltenes and Resins onto a Hydrophilic Surface. Colloidal and Interface Science 2002, 247(2), 342-350.

15. Farooq, U., Asif, N., Tweheyo, M.T., Sjoblom, J., and Qye, G. Effect of Low-Saline Aqueous Solutions and pH on the Desorption of Crude Oil Fractions from Silica Surfaces. Energy & Fuels 2011, 25, 2058-2064.

16. Farooq, Umer, Tweheyo, MT., et al. Surface Characterization of Model, Outcrop, and Reservoir Samples in Low Salinity Aqueous Solutions. Journal of Dispersion Science and Technology 2011, 32(4) 519-531.

17. Fathi, S.J., Austad, T. and Strand, S. and Puntervold, T. Wettability Alteration in Carbonates: The effect of Water-Soluble Carboxylic Acids in Crude Oil. Energy & Fuels 2010, 24, 2974-2979.

18. Fathi, S.J., Austad, T. and Strand, S. Water Based Enhanced Oil Recovery (EOR) by “Smart Water” in Carbonate Reservoirs. Conference of Oil and Gas West Asia, Muscat, Oman, 16-18 April 2012.

19. Gomari ,R. Different Approaches to Understand Mechanism of Wettability Alteration of Carbonate Reservoirs. SPE Europec/Eage Annual Conference and Exhibition, Amsterdam, Netherlands, 2009.

20. Guo, Y., Wang, D., Yang, L. and Liu, S. Nanoscale Monolayer Adsorption of Polyelectrolytes at the Solid/Liquid Interface Observed by Quartz Crystal Microbalance. Polymer Journal 2017, 49, 543-548.

21. Hognesen, E.J., Strand, S. and Austad, T. Water Flooding of Preferential Oil-Wet Carbonates: Oil Recovery Related to Reservoir Temperature and Brine Composition. Society of Petroleum Engineers 2005, doi: 10.2118/94166-MS.

22. Kanazawa, KK. and Gordon, G. Frequency of a Quartz Microbalance in Contact with Liquid. Analytical Chimica Acta, 1985, 175,99-105.

23. Karimi, M., Al-Maamari, R.S., Ayatollahi, S., and Mehranbod, N. Impact of Sulphate Ions on Wettability Alteration of Oil-Wet Calcite in the Absence and Presence of Cationic Surfactant. Energy *&* Fuels 2016, 30, 819-829.

24. Kasha, A., Al-Hashim, H., Abdallah, W., Taherian, R. and Sauerer, B. Effect of $Ca^{+2}$, $Mg^{+2}$ and $SO_4^{2-}$ Ions on the Zeta Potential of Calcite and Dolomite Particles Aged with Stearic Acid. Colloids and Surfaces A: Physicochemical and Engineering 2015, 482, 290-299.

25. Lager, A., Webb, K.J., Black, C.J.J., Singleton, M. and Sorbie, K.S. Low Salinity Oil Recovery-An Experimental Investigation1. Petrophysicists and Well Log Analysts 2008,49 (1).

26. Li, Jianyuan, Zhang, Z., Zhou, X., Chen, T., Nie, J. and Du, B. PNIPAmx–PPO36–PNIPAmx Thermo-Sensitive Triblock Copolymers: Chain Conformation and Adsorption Behavior on a Hydrophobic Gold Surface. Physical Chemistry Chemical Physics 2016, 18(1), 519-528.

27. Ligthelm, D., Gronsveld, J., Hofman, J. P., Brussee, N. J., Marcelis, F., & van der Linde, H. Novel Water Flooding Strategy by Manipulation of Injection Brine Composition. SPE Europec / Eage Annual Conference and Exhibition, Amsterdam, Netherlands, 2009.

28. Liu, X., Dedinaite, A., Nylander, T., Dabkowska, A.P, Skoda, M., Makuska, R., Calesson, P.M. Associated of Anionic Surfactant and Physisorbed Branched Brush Layers Probed by Neutron and Optical Reflectometry. Journal Colloid and Interface Science 2015, 440, 245-252.

29. Liu, X., Yan, W., Stenby, E.H., and Thormann, E. Release of Crude Oil from Silica and Calcium Carbonate Surfaces: On the Alternation of Surface and Molecular Forces by High-and Low-Salinity Aqueous Salt Solutions. Energy & Fuels 2016, 30,3986-3993.

30. Mahani , H. , Keya, A. L., Berg, S., and Nasralla The Effect of Salinity, Rock Type and pH on the Electrokinetics of Carbonate-Brine Interface and Surface Complexation Modeling. SPE Reservoir Characterization and Simulation Conference and Exhibition, Abu Dhabi, UAE, 2015.

31. McGuire, P.L., Chatham, J.R., Paskvan, F.K. Low Salinity Oil Recovery: An Exciting New EOR Opportunity for Alaska's North Slope. Irvine, California, USA, 2005, SPE-93903-MS.

32. Morrow, N., and Buckley, J. Improved Oil Recovery by Low-Salinity Water Flooding. JPT, May 2011,106-112.

33. Nasralla, R.A., Bataweel, M.A. and Nasr-El-Din, H.A. Investigation of Wettability Alteration by Low Salinity Water. In Offshore Europe, Aberdeen, UK, 2011.

34. Nasralla, R.A., Bataweel, M.A. and Nasr-El-Din, H.A. Investigation of Wettability Alteration and Oil-Recovery Improvement by Low-Salinity Water in Sandstone Rock. Journal of Canadian Petroleum Technology, 2013, 144-154.

35. Nourani, M., Tichelkamp, T., Gawel, B., Oye, G. Desorption of Crude Oil Components from Silica and Aluminosilicate Surfaces upon Exposure to Aqueous Low Salinity and Surfactant Solutions. Energy & Fuel 2016,180,1-6.

36. Pernyeszi, T., Patzko, A., Berkesi, O. And Dekany, I. Asphaltene Adsorption on Clays and Crude Oils Reservoir Rocks. Colloids and Surfaces A: Physicochemical and Engineering Aspects 1998,137 (3), 373-384.

37. Samanta, A., Ojha, K. and Mandal, A. Interactions between Acidic Crude Oil and Alkali and Their Effects on Enhanced Oil Recovery. Energy & Fuels 2011, 25, 1642-1649.

38. Sauerbrey,G.Z Phys . 1959. 155 (2), 206-222.

39. Sayyouh ,M.H. , Hemeida , A.M. , Al-Blehed ,M.S., Desouky ,S.M. Role of Polar Compounds in Crude Oils on Rock Wettability. Journal of Petroleum Science and Engineering 1991, 6 (3), 225-233.

40. Seccombe, J., Lager, A., Jerauld, G., Jhaveri, B., Buikema, T., Bassler, S., Denis, J., Webb, K.J, Cockin, A., Fueg, E. and Paskvan, F. Demonstration of Low-salinity EOR at Inter Well-Scale, Endicott Field, Alaska. SPE Improved Oil Recovery Symposium, Tulsa, Oklahoma, USA, 24-28 April 2010.

41. Speight, J.G The Chemistry and Technology of Petroleum, 5th edtion, CRC press, 2014.

42. Strand, S., Hognesen, E.J., and Austad, T. Wettability Alteration of Carbonates: Effects of Potential Determining Ions ($Ca^{+2}$ and $SO_4^{-2}$) and Temperature. Colloids and Surfaces A: Physicochemical and Engineering Aspects 2006, 275, 1-10.

43. Tang, G.O. and Morrow, N.R. Influence of Brine Composition and Fines Migration on Crude Oil / Rock Interactions and Oil Recovery. J.Pet.Science 1999, 24, 99-111.

44. Tapio, L., Subramanian, S., Simon,S. and Sjoblom,J Solvent Desorption of Asphaltenes from Solid Surfaces. Journal of Dispersion Science and Technology 2017, 38 (3), 355-360.

45. Vdović, Neda. Electrokinetic Behaviour of Calcite—The Relationship with Other Calcite Properties. Chemical Geology 2001,177(3),241-248.

46. Vledder, P., Fonseca, J.C., Wells, T., Gonzalez, I. and Ligthelm, D. Low Salinity Water Flooding: Proof of Wettability Alteration on a Field Wide Scale. SPE Improved Oil Recovery Symposium, Tulsa, Oklahoma, USA 24-28 April 2010.

47. Webb, K.J, Black, C.J.J and Al-Ajeel, H. Low Salinity Oil Recovery Log-Inject-Log. SPE/DOE Symposium on Improved Oil Recovery, Tulsa, Oklahoma, 17-21 April 2004.

48. Xie, K., Kuran, K. Kinetics and Thermodynamics of Asphaltene Adsorption on Metal Surfaces: A Preliminary Study. Energy & Fuels 2005,19 (4),1252-1260.

49. Xie, Q., Liu, Y., Wu, J. and Liu, Q. Ions Tuning Water Flooding Experiments and Interpretation by Thermodynamics of Wettability. Journal of Petroleum Science and Engineering 2014, 124, 350-358.

50. Yousef, A.A., Al-Saleh, S., Al-Kaabi,A. and Al-Jawfi, M. Laboratory Investigation of Injection-Water Salinity and Ionic Content on Oil Recovery from Carbonate Reservoirs. Society of Petroleum Engineers 2011, 578-593.

51. Zhang, P., Tweheyo, M.T., Austad, T. Wettability Alteration and Improved Oil Recovery in Chalk: The Effect of Calcium in the Presence of Sulfate. Energy & Fuels 2006, 20, 2056-2062.

52. Zhang, Y., Sie, X. and Morrow, N.R. Water Flooding Performance by Injection of Brine with Different Salinity for Reservoir Cores. SPE Annual Conference and Exhibition, California, CA, November 2007.